Application of metal–organic frameworks with coordinatively unsaturated metal sites in storage and separation of methane and carbon dioxide†

Pascal D. C. Dietzel,* Vasileios Besikiotis and Richard Blom

Received 9th June 2009, Accepted 6th August 2009
First published as an Advance Article on the web 21st August 2009
DOI: 10.1039/b911242a

The metal–organic frameworks $M_2(dhtp)(H_2O)_2 \cdot 8H_2O$ (CPO-27-M, M = Ni, Mg) can be activated to give the empty framework compounds $M_2(dhtp)$ with a honeycomb analogous structure containing large micropores of 11–12 Å diameter and a high concentration of open metal sites. These sites play a major role in the adsorption of methane and carbon dioxide, which was studied at pressures up to 100 bar and 50 bar, respectively, and various temperatures in the range of 179 to 473 K. Both gases are taken up by the material in significant amounts. The maximum excess adsorption of CO_2 observed at 298 K was 51 wt.% for $Ni_2(dhtp)$ and 63 wt.% for $Mg_2(dhtp)$. A surprisingly large amount of CO_2, in the range 25–30 wt.%, was still adsorbed at 473 K. Up to 18 and 22 wt.% methane were adsorbed at 179 K in the nickel and the magnesium compound, respectively. Congruent with this result is the high isosteric heat of adsorption observed, which was found to be in the range 38–43 kJ mol^{-1} for CO_2 and 20–22 kJ mol^{-1} for CH_4, initially. The heat of adsorption decreases significantly after the open metal sites have been occupied, which also is reflected in the shape of the adsorption isotherms. The vacant coordination site at the metal atom also imparts favorable properties in respect to gas separation onto the material. Breakthrough experiments using $Ni_2(dhtp)$ and gas mixtures of CO_2–N_2 and CO_2–CH_4 demonstrate the ability of the material to separate these gases. It is shown that carbon dioxide is preferentially adsorbed over methane or nitrogen. In the case of CO_2–N_2, the retention is quantitative within the precision of the detection system.

Introduction

The most costly step in carbon capture and sequestration (CCS) schemes is the CO_2 separation step.[1] At present, technologies available for separation at low partial pressures of CO_2 are scrubbing processes based on chemical solvents,[2] while separation at high CO_2 pressures are carried out by processes using so-called physical solvents.[3] Physical solvent-based processes for CO_2 removal from natural gas (gas sweetening) is regarded as mature technology, while chemical solvent-based processes have still not been demonstrated for full scale power plant applications. The latter are energy demanding due to relatively high regeneration temperatures and the large amount of water recycling needed. In addition, solvent-based processes might have negative environmental consequences in general due to solvent degradation and loss during operation. These factors necessitate a continuous search for more efficient and environmentally friendly ways to capture CO_2 from various gas streams. Processes based on adsorption on porous solids might be an attractive option.

SINTEF Materials and Chemistry, P.O. Box 124 Blindern, N-0314 Oslo, Norway. E-mail: pascal.dietzel@sintef.no; Fax: +47 22067350; Tel: +47 98243958

† Electronic supplementary information (ESI) available: Additional figures comparing the CO_2 and CH_4 adsorption in $Ni_2(dhtp)$ and $Mg_2(dhtp)$, isosteric heat of adsorption of CH_4 as function of loading, N_2 adsorption isotherms in $Ni_2(dhtp)$, and comparison of the amounts of CO_2, CH_4, and N_2 adsorbed in $Ni_2(dhtp)$. See DOI: 10.1039/b911242a

Metal–organic frameworks (MOFs) are a versatile substance class. The virtually infinite number of building blocks that can be employed in their construction can lead to structures and functional properties that make them useful in many different areas of application.[4–8] They are maybe best known for high surface areas and pore volumes. Consequently, the adsorption properties of MOFs have been among the most intensively studied of their properties.[9–14] A natural development has been the investigation of their ability to separate gases from each other.[15] The removal of carbon dioxide from mixtures with methane or nitrogen has been evaluated by calculating the selectivity on the basis of the single component adsorption isotherm[16–23] and/or by performing corresponding experiments.[24–29]

Recently, a series of isostructural compounds of composition $M_2(dhtp)(H_2O)_2 \cdot 8H_2O$ (denominated CPO-27-M by us and MOF-74 for the zinc compound by Rosi *et al.*;[30] CPO: Coordination Polymer of Oslo; M = Ni, Co, Zn, Mg, Mn) has been prepared from various metal precursors and 2,5-dihydroxyterephthalic acid (H_4dhtp).[30–34] The structure is honeycomb-like with large one-dimensional pores of ~11–12 Å diameter. The solvent contained in the channels after synthesis is easily removed by thermal treatment, resulting in an activated stable framework structure. A characteristic feature of the structure of the activated $M_2(dhtp)$ framework compound is the presence of a high concentration of coordinatively unsaturated metal cations (Fig. 1).[32,33,35] This vacant coordination site at the metal ion is the primary coordination site for guest molecules, as has been shown in a number of diffraction studies involving various host–guest combinations.[36–38] As can be assumed from the Lewis acid nature

 This journal is © The Royal Society of Chemistry 2009

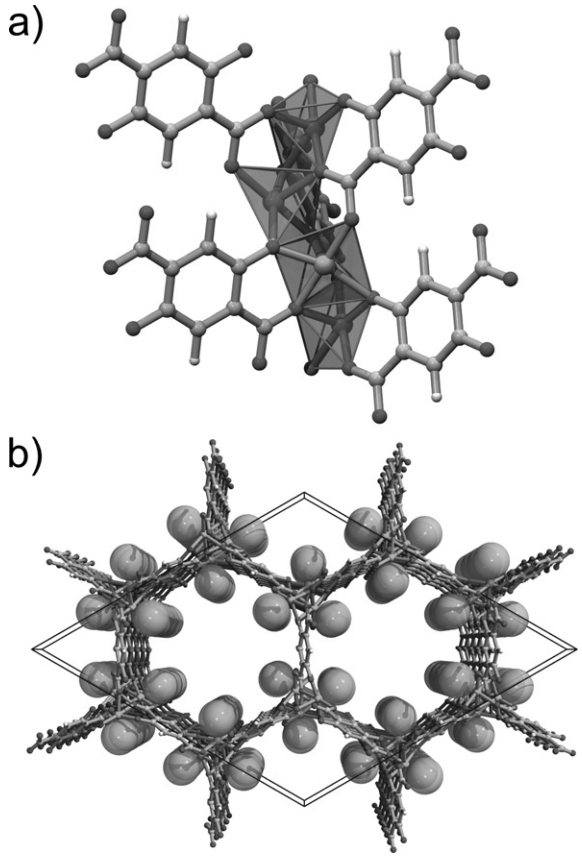

Fig. 1 (a) Cutout along the chains of metal–organic framework CPO-27 showing the coordinatively unsaturated metal site in form of the square-pyramidally coordinated metal atom; (b) Crystal structure of CPO-27 viewed along the channels illustrating the primary adsorption site at the metal as large spheres.

of the metal cation, there is generally strong interaction between the metal and molecules which can act as Lewis base, *e.g.* water, CO_2, NO, and CO leading to defined adducts in which a coordinative bond has formed between the guest molecule and the metal cation.[36,39–41] Furthermore, strong interaction between the metal ion and hydrogen, a molecule not possessing free electron pairs that it might donate towards the Lewis acidic centre, has been observed.[33,38,40,42] This is probably a result of increased dispersion forces at work between the cation and the polarizable hydrogen molecule. Non-negligible interaction can therefore be expected for other non-Lewis base molecules, methane being one example.

In this report, we present the results of adsorption studies on the nickel and magnesium members of the CPO-27-M series. The nickel compound was selected because of the facility with which it can be activated, while the magnesium compound represents the coordination polymer of this non-toxic lightweight metal with the highest specific surface area to date.

Experimental

Synthesis of materials

CPO-27-Ni. A solution of 2,5-dihydroxyterephthalic acid (2.972 g, 15 mmol) in THF (50 mL) and a solution of nickel(II) acetate tetrahydrate (7.466 g, 30 mmol) in water (50 mL) were combined in a Teflon-lined insert of 200 mL volume. The insert was put into an autoclave, sealed, and reacted for 3 days at 383 K in a pre-heated furnace. Filtration yields 6.461 g of a yellowish fine crystalline product which was washed three times with water (50–100 mL). Powder X-ray diffraction confirms the identity of the compound.

CPO-27-Mg. Magnesium acetate tetrahydrate (3.216 g, 15 mmol), 2,5-dihydroxyterephthalic acid (1.486 g, 7.5 mmol), *N*-methylpyrrolidone (90 mL), and water (10 mL) are combined in the 200 mL Teflon insert of an autoclave. After homogenization of the mixture, the autoclave is sealed and reacted at 393 K for 1 day. Filtration and washing with methanol yields 1.502 g of a bright yellow fine crystalline compound. Powder X-ray diffraction confirms the identity of the compound.

Gas adsorption measurements

The porosity of the as-synthesized materials was confirmed by nitrogen adsorption measurements at 77 K using a BELSORP-max instrument. As-synthesized CPO-27-Ni was pre-treated by heating at 473 K for 19 h in dynamic vacuum using an external pre-treatment station and at 383 K for 1 h connected to the adsorption instrument. An apparent BET surface area of 1218 $m^2\ g^{-1}$ and pore volume of 0.47 $cm^3\ g^{-1}$ was obtained. CPO-27-Mg was treated with methanol for 7 d. The solvent was exchanged once per day. It was then pre-treated by heating at 513 K for 48 h in a dynamic vacuum at the external station and 1 h at 393 K connected to the adsorption instrument. All operations were performed under an inert atmosphere. An apparent BET surface area of 1542 $m^2\ g^{-1}$ and pore volume of 0.63 $cm^3\ g^{-1}$ was obtained. Comparison of the experimentally derived pore volumes with calculation of the void space in the empty crystal structure indicates that the materials were essentially fully activated. Calculations were performed using PLATON[43] and yielded a theoretical pore volume of 0.48 $cm^3\ g^{-1}$ for Ni_2(dhtp) and 0.65 $cm^3\ g^{-1}$ for Mg_2(dhtp).

High pressure gas adsorption isotherms at pressures up to 10 000 kPa were measured using a Belsorp-HP instrument equipped with an additional higher precision pressure transducer for the pressure range below 100 kPa. Ultrahigh purity grade carbon dioxide (99.9992%), methane (99.9995%), nitrogen (99.999%), and helium (99.9999%) were used. The dead volume of the empty sample cell was determined at 298 K using helium gas prior to filling with the sample. Prior to measurement, CPO-27-Ni was pre-treated for 12 h at 473 K in a dynamic vacuum, resulting in 1.266 g of activated sample. CPO-27-Mg was pre-treated for 19 h at 523 K in a dynamic vacuum, yielding 0.477 g of activated sample.

The non-ideal behaviour of the gas was corrected for by application of virial equations employing four virial coefficients. The equations were obtained by fitting the polynomal equation to the pressure dependent compressibility factor Z, which was calculated from NIST data.[44] The experimental data of the volume of CO_2 and CH_4 adsorbed are shown in Fig. S1 and Fig. S2 in the ESI.†

Isosteric heats of adsorption were calculated using the adsorption isotherms collected at the lowest available

temperatures, corresponding to the highest observed levels of loading, specifically 278 and 298 K for CO_2, and 179 and 283 K for CH_4.

Gas separation experiments

The experimental setup consisted of two fixed bed glass reactors with an inner diameter of 4.6 mm which are connected in parallel. The reactors can be fed intercommunicably with an inert gas (helium) or the probe gas by switching a four-way valve. One reactor was loaded with the adsorbent (typically 500 mg), while the other reactor contained compact glass spheres having the same particle size distribution (90–210 μm) as the adsorbent particles. The dead volume of the setup was minimized by filling with compact glass spheres to make the total volume of the dummy reactor and the adsorbing reactor as similar as possible. The effluent gas from the adsorbing reactor was monitored continuously by mass spectrometric (MS) analysis. Prior to the breakthrough experiment, the sample was activated by flushing the reactor containing the adsorbent with inert gas at 423 K for 2 h. Subsequently, the reactor was allowed to equilibrate at the measurement temperature before the gas feeds were switched. Breakthrough curves using gas mixtures of 40% CO_2 in CH_4 and 40% CO_2 in N_2 were collected at 323 and 353 K using a total gas flow of 20 cm^3 min^{-1} (GHSV = 2400 h^{-1}).

Results and discussion

Carbon dioxide adsorption

Recent investigations of the carbon dioxide adsorption in these framework materials at up to atmospheric pressure have shown a significant uptake at ambient temperature.[36,45] We have confirmed previously by crystal structure determination from powder data that the carbon dioxide molecule is indeed coordinating the metal cation in an end-on fashion through one of its oxygen atoms.[36] Caskey *et al.* have compared the various CPO-27 materials, finding that the magnesium compound surpassed the other members of the isostructural series in CO_2 adsorption

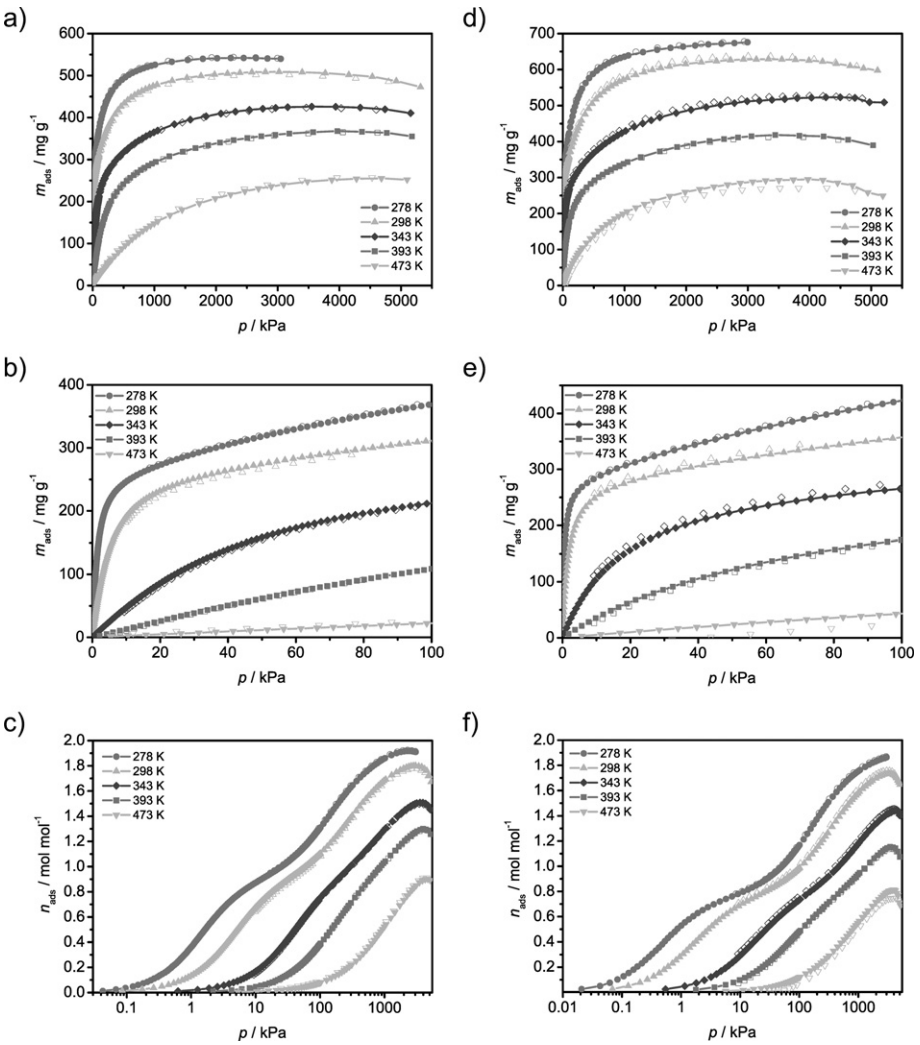

Fig. 2 Excess carbon dioxide adsorption (filled symbols) and desorption (open symbols) isotherms for CPO-27-Ni (left) and Mg (right) at various temperatures: sorption in mass units in the full pressure range (a and d) and as excerpt in the pressure range up to 100 kPa (b and e), number of molecules adsorbed per formula unit/metal atom (e and f).

This journal is © The Royal Society of Chemistry 2009

at 296 K and 100 kPa.[45] The effect was not only due to the lighter weight of the metal. The Mg compound actually had a higher heat of adsorption and took up more CO_2 molecules per unit cell than its analogues in the low pressure range. In extension of these prior reports, we performed adsorption experiments using CO_2 at temperatures of 278, 298, 343, 393, and 473 K and at pressures up to 5000 kPa (Fig. 2). We expect the wider temperature and pressure range at which these measurements are performed will aid in the evaluation of the materials for application as adsorbents.

A significant amount of carbon dioxide is already taken up at low pressures in the activated CPO-27 materials studied here at ambient temperatures. In Ni_2(dhtp), the maximum adsorption at 278 K is 54.2 wt% at 2200 kPa (corresponding to 1.92 molecules CO_2 per Ni atom and 34.5 molecules CO_2 per unit cell, respectively); 50 wt% are already adsorbed at 580 kPa. In fact, the first half of the CO_2 uptake occurs below 20 kPa. The adsorption curve follows similar trends at 298 K, with only a slightly reduced maximum adsorption of 50.9 wt%. The maximum amount of adsorbed CO_2 decreases further upon further increase of the temperature. It reaches 42.6 wt% at 3550 kPa and 343 K, 36.8 wt% at 3970 kPa and 393 K, and 25.5 wt% at 4680 kPa and 473 kPa. The adsorption isotherms of CO_2 on Mg_2(dhtp) look similar to the ones of its nickel analogue. The lighter weight of the material is reflected in the fact that the corresponding values of adsorption in weight percent are larger. Thus, Mg_2(dhtp) adsorbs up to 68.9 wt% at 3600 kPa and 278 K (corresponding to 1.9 molecules CO_2 per Mg atom, or 34 molecules CO_2 per unit cell, respectively), 62.9 wt% at 3300 kPa and 298 K, 52.3 wt% at 4500 kPa and 343 K, 41.8 wt% at 3440 kPa and 393 K, and 29.5 wt% at 3980 kPa and 473 K. We find that while the mass uptake is higher for the magnesium compound than for the nickel compound, the actual amount of carbon dioxide adsorbed is roughly equal for both compounds (Fig. 2c and 2f and Fig. S3, ESI†), approaching two molecules of CO_2 per metal (*i.e.* 36 molecules per unit cell). This appears reasonable on the basis that the volume available to be filled by guest molecules is approximately the same for the isostructural compounds.

We can derive the change in available pore volume upon adsorption of CO_2 in Ni_2(dhtp) on the basis of our previous crystal structure determinations of the empty Ni_2(dhtp) framework compound and of the CO_2 adduct.[33,36] Calculation of the void space using PLATON[43] yields a pore volume of 2240 Å^3 within the unit cell volume of 3898 Å^3, *i.e.* 58% of the crystal structure is empty space. After adsorption of one CO_2 molecule at the open metal site, the void volume has decreased to 1466 Å^3 within a unit cell volume 3885 Å^3. (Note that the occupancy factor of CO_2 coordinating the cation was only 2/3 in the actual crystal structure determination. We set the occupancy to unity for the purpose of this calculation.) Thus, the pore volume has diminished by approximately 1/3. It still amounts to 38% of the structure. Consequently, there should be sufficient space available in the structure to allow facile diffusion and adsorption of additional molecules. Fast diffusion to pertinent adsorption sites are a crucial point for use of the material as a selective adsorbent in separation.

At 278 K, a pronounced inflection[46] is observed in the adsorption isotherm upon approach of one adsorbed molecule of carbon dioxide per metal cation (Fig. 2c and f). The bend in the curve becomes less pronounced with increasing temperature. It is caused by the difference in isosteric heat of adsorption between the primary adsorption site at the metal cation and subsequently occupied adsorption sites. The first molecule, which is adsorbed at the vacant coordination site of the metal cation, experiences a significantly larger isosteric heat of adsorption than the subsequent molecule (Fig. 3). The heat of adsorption for the CO_2 molecule at the magnesium cation is several kJ mol^{-1} larger than for the nickel cation. Consequently, Mg_2(dhtp) adsorbs CO_2 more readily at low pressures than Ni_2(dhtp) (Fig. S3, bottom, ESI†). However, once most of these primary adsorption sites have been occupied and pore filling commences, Ni_2(dhtp) takes up additional carbon dioxide more readily, which is also reflected in the fact that the isosteric heats of adsorption as a function of loading cross each other (Fig. 3). The point of inflection where the slope of the adsorption curve increases again corresponds to ~0.92 CO_2–Ni and ~0.78 CO_2–Mg at 278 K. This difference may indicate that not all of the metal sites are equally easily accessible within the material, be that because of a reduced rate of diffusion at such loadings or because the remaining metal sites are physically obstructed from access because of defects in the crystal structure.

The maximum uptake of carbon dioxide at 473 K is astonishingly high for both compounds, reaching 26 wt% for Ni_2(dhtp) and 30 wt% for Mg_2(dhtp). To the best of our knowledge, this is the first time such significant values have been reported for MOFs at this high temperature. More important possibly is the fact that the slope of the adsorption curve becomes gradually less steep with increasing temperature, reaching a form potentially suitable for pressure swing adsorption processes between 393 K and 473 K. In the PSA process, an as high as possible difference in adsorption capacity is desired within the pressure range in which the process is most economical, which often is between 500 and 2000 kPa. Ni_2(dhtp) can adsorb and desorb reversibly ~11 wt% at 473 K in this range, while it is only ~7 wt% at 298 K. At 473 K, Mg_2(dhtp) adsorbs only slightly more CO_2, 11.7 wt%, than Ni_2(dhtp) between 500 and 2000 kPa. In our experience, CPO-27-Ni can be easily handled in ambient conditions, possibly making this the material of choice.

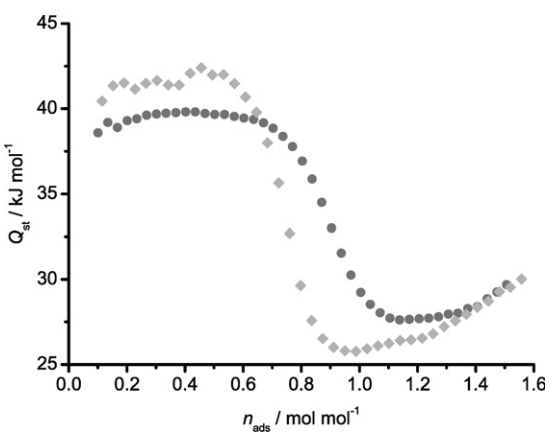

Fig. 3 Isosteric heat of adsorption of CO_2 on Ni_2(dhtp) (dark grey) and Mg_2(dhtp) (light grey) relative to the amount of metal atoms.

Methane adsorption

Adsorption isotherms of methane on Ni_2(dhtp) and Mg_2(dhtp) were performed at 179, 283, 298, 313, and 343 K and pressures up to 10 000 kPa (Fig. 4). While this manuscript was under preparation, Wu *et al.* reported a comparison of the methane adsorption properties of the M_2(dhtp) (M = Ni, Co, Zn, Mg, Mn) series, with adsorption isotherms collected at 270, 280, and 298 K.[47] We essentially confirm the results by Wu *et al.* and extend on their measurements.

At 179 K, a maximum uptake of 17.8 wt% at 1000 kPa was observed for Ni_2(dhtp) (corresponding to 1.73 molecules CH_4 per Ni atom, or 31 molecules CH_4 per unit cell, respectively). This decreased to 12.7 wt% at 4620 kPa and 283 K, 11.9 wt% at 4970 kPa at 298 K, and 10.0 wt% at 6840 kPa and 343 K. The corresponding values for Mg_2(dhtp) are 22.2 wt% at 1690 kPa and 179 K (corresponding to 1.68 molecules CH_4 per Mg atom, or 30 molecules CH_4 per unit cell, respectively), 14.6 wt% at 5060 kPa and 283 K, 13.7 wt% at 5830 kPa and 298 K, 12.9 wt% at 5890 kPa and 313 K, and 11 wt% at 7040 kPa and 343 K. The U.S. Department of Energy has defined a target of 180 cm^3(STP) per cm^3 at 3500 kPa and 298 K for the capacity of a methane storage material. On the basis of the crystallographic density of the empty MOF framework compounds, Ni_2(dhtp) exceeds this value (with 195 cm^3(STP) per cm^3), while Mg_2(dhtp) comes close (with 169 cm^3(STP) per cm^3). In fact, the storage capacity of the DOE target is already reached by Ni_2(dhtp) at 2000 kPa. At lower temperature, both materials surpass this amount by far. At 179 K, Ni_2(dhtp) and Mg_2(dhtp) already have a capacity of 259 and 229 cm^3(STP) per cm^3), respectively, at 100 kPa. It further increases to a maximum of 297 cm^3(STP) per cm^3 at 1020 kPa and 284 cm^3(STP) per cm^3 at 1690 kPa for the nickel and the magnesium compound, respectively. A comparison of the density of methane reached by adsorption in the M_2(dhtp) compounds with that of liquid methane at the boiling point (0.415 g cm^{-3}) might be enlightening regarding the aptitude of the material as a storage material for methane. Liquified natural gas (LNG) consists predominantly of methane and is transported on a large

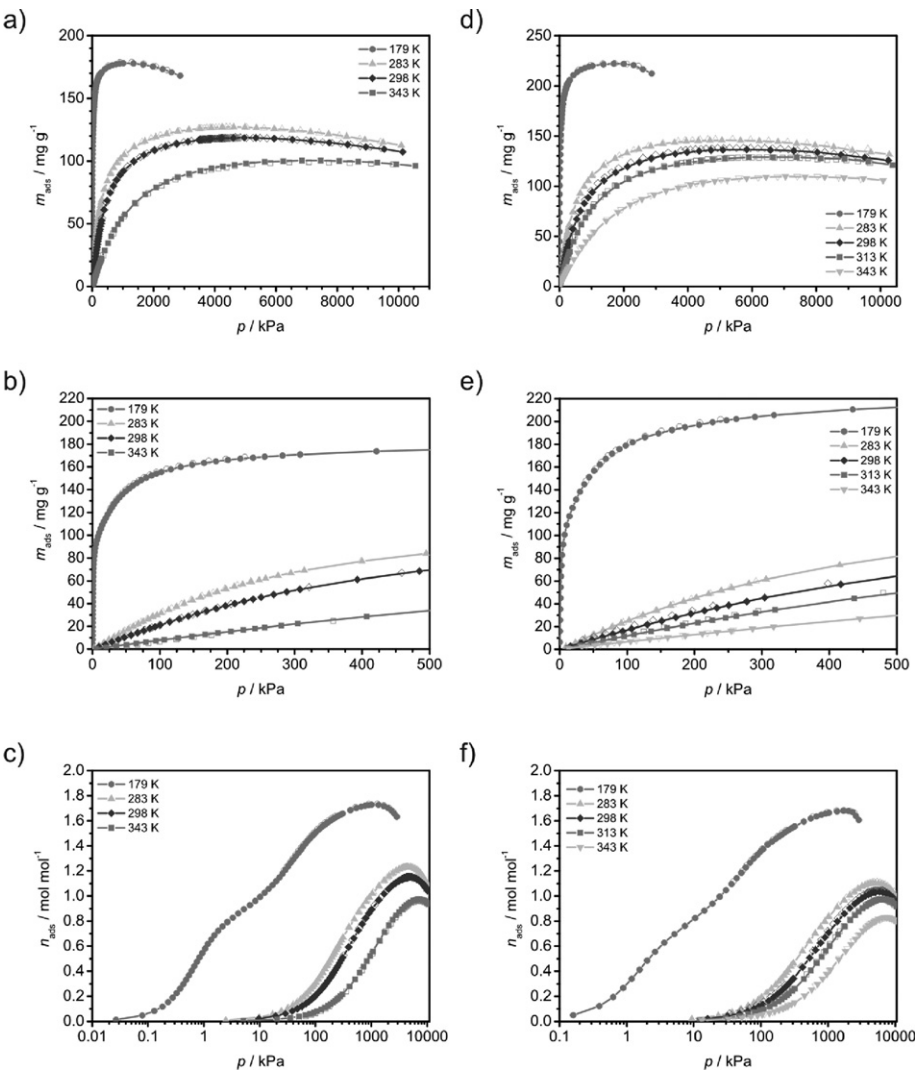

Fig. 4 Excess methane adsorption (filled symbols) and desorption (open symbols) isotherms for CPO-27-Ni (left) and Mg (right) at various temperatures: sorption in mass units in the full pressure range (a and d) and as excerpt in the pressure range up to 500 kPa (b and e), number of molecules adsorbed per formula unit/metal atom (e and f).

 This journal is © The Royal Society of Chemistry 2009

scale at close to atmospheric pressure at approximately 110 K. In contrast to the adsorption of CO_2, Ni_2(dhtp) takes up more CH_4 molecules than Mg_2(dhtp) in the full pressure range investigated (Fig. S4, ESI†). Since the unit cell volume of both compounds is of similar value, the methane stored in the nickel compound therefore will also have a higher density than methane stored in the magnesium compound. However, the difference is relatively small, *e.g.* at 100 kPa and 179 K, the CH_4 density will be 0.186 and 0.164 g cm^{-3} (corresponding to 45% and 40% of the density of liquid methane at the boiling point) in Ni_2(dhtp) and Mg_2(dhtp), respectively. This evaluation does not take the more significant weight difference of the storage material into account, which will favor the magnesium compound. Still, a transport vessel with a given volume of storage space will only be able to transport less than half the amount of methane using the MOFs at 100 kPa and 179 K. The temperature would be higher than in current LNG transport conditions, but cooling is still required. Thus, it stands to reason that it will not be cost effective to use the materials as methane storage materials at atmospheric pressure and temperatures requiring additional refrigeration equipment. On the other hand, at 298 K and 3500 kPa, both materials easily store methane corresponding to 30–35% of the density of liquid methane at 112 K. In this case, applicability will be determined by the balance between the benefit of removing the cooling system and the cost due to the additional weight of the adsorbent and the effort of using pressurized containers.

The larger uptake of CH_4 in Ni_2(dhtp) over Mg_2(dhtp) is also reflected by the isosteric heats of adsorption, which are continuously 1–2 kJ mol^{-1} larger for the nickel compound than for the magnesium analogue in the range covered (Fig. S5, ESI†). They lie in the 20–22 kJ mol^{-1} range initially, and decrease to ~18.5 kJ mol^{-1} upon approach of full occupancy of the open metal site. Wu *et al.* have shown in the example of Mg_2(dhtp) that the primary adsorption site of the methane molecule is indeed the coordinatively unsaturated metal atom.[47] Because only up to ~1 molecule CH_4 per metal cation is adsorbed at 283 K, which is the higher temperature isotherm used for the calculation of Q_{st}, the calculation does not yield values for $n_{ads} > 1$. However, one can infer from analogy with the trend observed for CO_2 that the end point of the decrease has been reached at $n_{ads} = 1$. The initial heat of adsorption at the open nickel site is then in the range of 21.5–22 kJ mol^{-1}, while the heat of adsorption at the secondary adsorption site lies initially in the 18–19 kJ mol^{-1} range and may further increase upon progressive loading. In any case, the heat of adsorption of methane in both M_2(dhtp) materials is more than 50% larger than in MOF-5 and ZIF-8.[48]

Nitrogen adsorption relative to CO_2 and CH_4 adsorption

Nitrogen adsorption isotherms were collected for Ni_2(dhtp) at 298, 313, 343, 393, and 473 K at up 10 000 kPa (Fig. S4, ESI†). Comparison with the uptake of carbon dioxide and methane allows a preliminary evaluation whether the material might preferably adsorb one of these components from the others in a gas mixture (Fig. 5 and Fig. S6, ESI†).

It is easily apparent that CO_2 is the strongest adsorbing of the three gases, showing significantly higher uptakes than the other two. Almost 7 times more CO_2 molecules are adsorbed in Ni_2(dhtp) at 298 K and 100 kPa than N_2 molecules. The ratio increases to 15 for 343 K and 100 kPa and 16 for 393 K and 100 kPa, before decreasing again to 9 for 473 K and 100 kPa. The ratio can be dramatically larger at lower than atmospheric pressures. In general, we found a larger amount of methane than nitrogen was adsorbed at all temperatures for which data for both adsorbates is available.

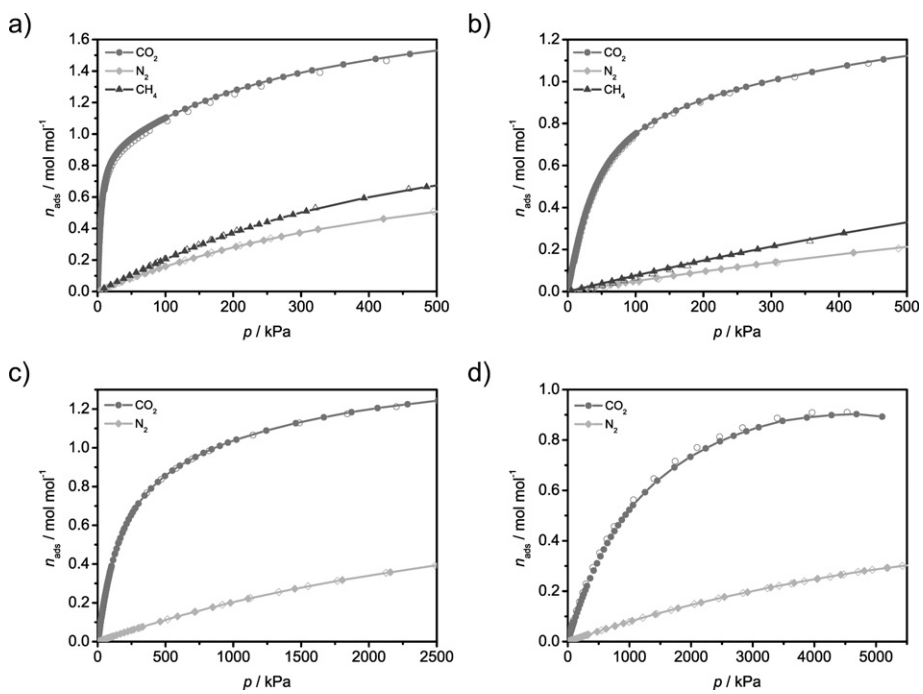

Fig. 5 Amounts adsorbed of CO_2, CH_4, and N_2 relative to amount of metal sites in Ni_2(dhtp) at 298 (a), 343 (b), 393 (c), and 473 K (d). (For the full pressure range see Fig. S7, ESI†).

This comparison already indicates that one might expect good selectivity of Ni_2(dhtp) for the competitive adsorption of carbon dioxide in mixtures with nitrogen, and a somewhat diminished degree of separation in mixtures with methane.

Gas separation properties

The M_2(dhtp) materials take up more molecules of carbon dioxide than methane or nitrogen at a given pressure (and temperature). Accordingly, the heat of adsorption of carbon dioxide in the materials is significantly larger than that for methane or nitrogen. On the basis of these results from the single component isotherms one can expect that the compounds will also show preferential adsorption of carbon dioxide over nitrogen or methane in a binary mixture, making these potentially useful materials in carbon dioxide separation from real gas streams. As it is by and large the presence of the open metal site which imparts this selectivity on the material, the high concentration of such sites in M_2(dhtp) (dhtp = $C_8H_2O_6$) should directly benefit its performance. We tested this hypothesis by performing breakthrough measurements with Ni_2(dhtp) using CO_2–CH_4 and CO_2–N_2 gas mixtures at 323 K and 353 K at ambient pressure. The dead volume, including the pore space of the framework compound, of the reactor containing the activated Ni_2(dhtp) material was occupied with helium as a consequence of the pre-treatment procedure before the gas feed was switched to the binary gas mixture. Using a 40 : 60 CO_2–N_2 mixture at 323 K (Fig. 6a), an immediate sharp drop in concentration of both, CO_2 and N_2, is observed upon switching the gas feed. Both gases are apparently adsorbed on the MOF, while the helium inside is being displaced. Carbon dioxide continues to be adsorbed almost quantitatively (to well below 0.5%). The N_2 level in the exhaust gas, on the other hand, quickly increases again after the initial dip to levels above its feed level, indicating that the amount captured by the activated MOF is being replaced by CO_2. Subsequently, all three gases remain at approximately constant levels for as long as the adsorbent has enough capacity to essentially adsorb all the CO_2 from the gas feed entering the reactor. Finally, the level of CO_2 begins to increase again ~2.3 min after switching the gas feeds. At this point in time, an amount of CO_2 has been captured by the adsorbent corresponding to approximately 25% of the available open metal sites. The total amount adsorbed corresponds to ~45% of the metal cations. The picture looks similar at 353 K (Fig. 6c) and otherwise identical conditions. Carbon dioxide is at first essentially completely adsorbed by the metal–organic framework. Nitrogen is initially adsorbed but quickly replaced by CO_2. However, the higher temperature results in breakthrough occurring much faster. The level of CO_2 in the exhaust gas begins to increase again after only ~6% of the open metal sites are occupied by carbon dioxide, and the overall capacity corresponds to roughly 25% of metal sites hypothetically available.

The selectivity of Ni_2(dhtp) to adsorb CO_2 rather than N_2 was sufficiently high at both temperatures to lead to initially complete removal of the CO_2 from the gas stream. This aptitude of the material to adsorb CO_2 is somewhat reduced when the second gas is methane instead of nitrogen. As was discussed above, the amount of methane that was adsorbed at identical pressures was larger than that of nitrogen, and this already indicated the selectivity might be worse. Still, the material captures most of the CO_2 from the gas feed at 323 K for some time, while breakthrough occurs quickly at 353 K (Fig. 6b and d). It was easily possible in all cases to desorb the carbon dioxide again by flowing inert gas through the column containing the adsorbent and increasing the temperature. Most of the sorbate is actually released by the simple change of atmosphere at the temperatures we performed the experiments at.

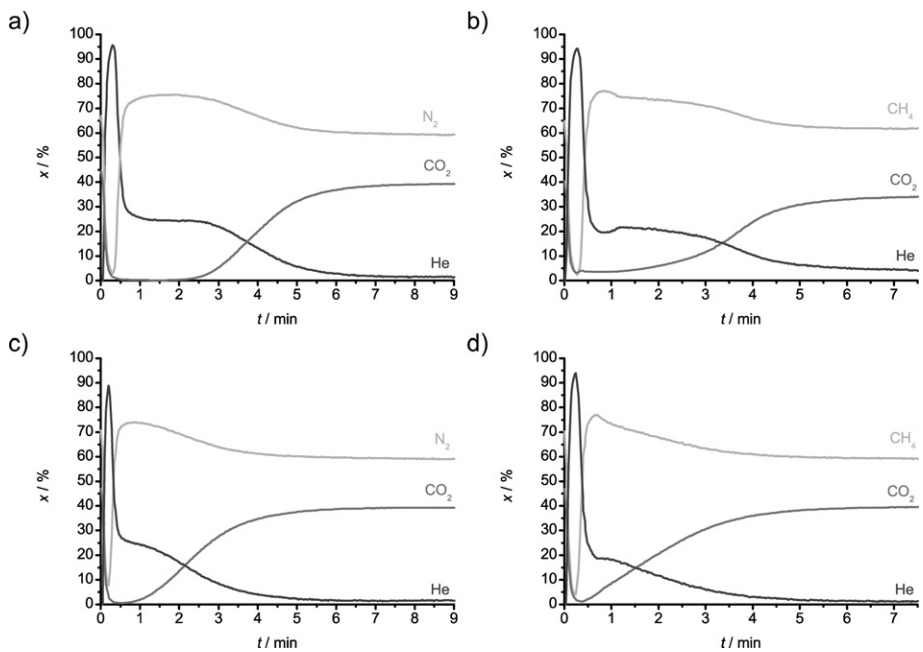

Fig. 6 Breakthrough curves from gas separation experiments with Ni_2(dhtp) using mixtures of 40% CO_2 and 60% N_2 and a flow rate of 20 cm^3 min^{-1} at 323 K (a) and 353 K (c) and of 40% CO_2 and 60% CH_4 at 323 K (b) and 353 K (d).

 This journal is © The Royal Society of Chemistry 2009

The experiments have clearly demonstrated the ability of Ni_2(dhtp) to capture CO_2 preferentially over nitrogen and methane. The performance in respect to CO_2–N_2 separation was better than for CO_2–CH_4 separation. However, for both gas mixtures, a significant improvement is expected at lower temperatures, *e.g.* room temperature, which will further favor physisorption of CO_2 at the open metal site in respect to kT, as can be seen by comparing the actually used capacity with respect to the amount of coordination sites available for CO_2–N_2 at 323 and 353 K.

While Ni_2(dhtp) showed a strong selectivity towards CO_2 in the above experiments, it was also facile to remove it again from the solid sorbent. It should therefore be possible to efficiently remove carbon dioxide from mixtures with nitrogen and methane in a continuous manner by parallelizing several reactors and using them in turn as adsorbent while the remainder is being regenerated.

Conclusions

The activated compounds of the CPO-27-M series contain a large amount of open metal sites which impart a high affinity towards adsorption of guest molecules onto the materials. Large amounts of methane and carbon dioxide have been shown to be adsorbed in Ni_2(dhtp) and Mg_2(dhtp). Uptakes of more than 50 wt% were observed at 298 K at high pressure. Significant amounts of 25–30 wt% CO_2 were still adsorbed at such elevated temperatures as 473 K, indicating possible use of the materials in processes necessitating higher temperatures. The isosteric heat of adsorption shows a clear trend. It is significantly higher for the first molecule of CO_2 which is adsorbed on the metal site than for adsorption surpassing this amount. Mg_2(dhtp) and Ni_2(dhtp) also approach or exceed, respectively, the DOE target for methane storage at 298 K and 3500 kPa. The adsorption capacity is even larger at lower temperatures. At 179 K and 100 kPa, the density of methane was found to be in the range of 40–45% of the density of liquid methane at the boiling point. The relative amounts of molecules adsorbed were compared for CO_2, CH_4, and N_2. These indicate a strong preference for the adsorption of CO_2. This was ultimately demonstrated in breakthrough experiments using Ni_2(dhtp) and realistic 40% CO_2 and 60% CH_4 or N_2 mixtures. Within the precision of the detection system, quantitative separation of CO_2 from N_2 and substantial retention of CO_2 in mixtures with CH_4 was observed. As a consequence, the material may be eminently suitable for application in separation processes.

Acknowledgements

The financial support of the Research Council of Norway through the NANOMAT program (grant 182056/S10) and the European Union (NMP project "MOFCAT", grant 033335, and Energy project "DECARBit", grant 211971) is gratefully acknowledged.

Notes and references

1 R. Steeneveldt, B. Berger and T. A. Torp, *Chem. Eng. Res. Des.*, 2006, **84**, 739.
2 A. B. Rao and E. S. Rubin, *Environ. Sci. Technol.*, 2002, **36**, 4467.
3 G. Astarita, D. W. Savage and A. Bisio, *Gas Treating with Chemical Solvents*, Wiley, New York, 1983.
4 A. K. Cheetham, C. N. R. Rao and R. K. Feller, *Chem. Commun.*, 2006, 4780–4795.
5 G. Férey, *Chem. Soc. Rev.*, 2008, **37**, 191–214.
6 C. Janiak, *Dalton Trans.*, 2003, 2781–2804.
7 S. Kitagawa, R. Kitaura and S. Noro, *Angew. Chem., Int. Ed.*, 2004, **43**, 2334–2375.
8 S. Kitagawa, S. Noro and T. Nakamura, *Chem. Commun.*, 2006, 701–707.
9 A. J. Fletcher, K. M. Thomas and M. J. Rosseinsky, *J. Solid State Chem.*, 2005, **178**, 2491–2510.
10 R. E. Morris and P. S. Wheatley, *Angew. Chem., Int. Ed.*, 2008, **47**, 4966–4981.
11 K. M. Thomas, *Dalton Trans.*, 2009, 1487–1505.
12 D. Zhao, D. Yuan and H.-C. Zhou, *Energy Environ. Sci.*, 2008, **1**, 222–235.
13 S. S. Han, J. L. Mendoza-Cortés and W. A. Goddard III, *Chem. Soc. Rev.*, 2009, **38**, 1460–1476.
14 L. J. Murray, M. Dincă and J. R. Long, *Chem. Soc. Rev.*, 2009, **38**, 1294–1314.
15 J.-R. Li, R. J. Kuppler and H.-C. Zhou, *Chem. Soc. Rev.*, 2009, **38**, 1477–1504.
16 R. Babarao, J. Jiang and S. I. Sandler, *Langmuir*, 2009, **25**, 5239–5247.
17 Y.-S. Bae, O. K. Farha, A. M. Spokoyny, C. A. Mirkin, J. T. Hupp and R. Q. Snurr, *Chem. Commun.*, 2008, 4135–4137.
18 Y.-S. Bae, K. L. Mulfort, H. Frost, P. Ryan, S. Punnathanam, L. J. Broadbelt, J. T. Hupp and R. Q. Snurr, *Langmuir*, 2008, **24**, 8592–8598.
19 S. Cavenati, C. A. Grande, A. E. Rodrigues, C. Kiener and U. Müller, *Ind. Eng. Chem. Res.*, 2008, **47**, 6333–6335.
20 S. Keskin and D. S. Sholl, *J. Phys. Chem. C*, 2007, **111**, 14055–14059.
21 S. Keskin and D. S. Sholl, *Ind. Eng. Chem. Res.*, 2009, **48**, 914–922.
22 B. Mu, F. Li and K. S. Walton, *Chem. Commun.*, 2009, 2493–2495.
23 A. Ö. Yazaydın, A. I. Benin, S. A. Faheem, P. Jakubczak, J. J. Low, R. R. Willis and R. Q. Snurr, *Chem. Mater.*, 2009, **21**, 1425–1430.
24 R. Banerjee, H. Furukawa, D. Britt, C. Knobler, M. O'Keeffe and O. M. Yaghi, *J. Am. Chem. Soc.*, 2009, **131**, 3875–3877.
25 P. S. Bárcia, L. Bastin, E. J. Hurtado, J. A. C. Silva, A. E. Rodrigues and B. Chen, *Sep. Sci. Technol.*, 2008, **43**, 3494–3521.
26 L. Bastin, P. S. Bárcia, E. J. Hurtado, J. A. C. Silva, A. E. Rodrigues and B. Chen, *J. Phys. Chem. C*, 2008, **112**, 1575–1581.
27 S. Couck, J. F. M. Denayer, G. V. Baron, T. Rémy, J. Gascon and F. Kapteijn, *J. Am. Chem. Soc.*, 2009, **131**, 6326–6327.
28 V. Finsy, L. Ma, L. Alaerts, D. E. De Vos, G. V. Baron and J. F. M. Denayer, *Microporous Mesoporous Mater.*, 2009, **120**, 221–227.
29 B. Wang, A. P. Côté, H. Furukawa, M. O'Keeffe and O. M. Yaghi, *Nature*, 2008, **453**, 207–212.
30 N. L. Rosi, J. Kim, M. Eddaoudi, B. Chen, M. O'Keeffe and O. M. Yaghi, *J. Am. Chem. Soc.*, 2005, **127**, 1504–1518.
31 P. D. C. Dietzel, R. Blom and H. Fjellvåg, *Eur. J. Inorg. Chem.*, 2008, 3624–3632.
32 P. D. C. Dietzel, Y. Morita, R. Blom and H. Fjellvåg, *Angew. Chem., Int. Ed.*, 2005, **44**, 6354–6358.
33 P. D. C. Dietzel, B. Panella, M. Hirscher, R. Blom and H. Fjellvåg, *Chem. Commun.*, 2006, 959–961.
34 W. Zhou, H. Wu and T. Yildirim, *J. Am. Chem. Soc.*, 2008, **130**, 15268–15269.
35 P. D. C. Dietzel, R. E. Johnsen, R. Blom and H. Fjellvåg, *Chem.–Eur. J.*, 2008, **14**, 2389–2397.
36 P. D. C. Dietzel, R. E. Johnsen, H. Fjellvåg, S. Bordiga, E. Groppo, S. Chavan and R. Blom, *Chem. Commun.*, 2008, 5125–5127.
37 A. C. McKinlay, B. Xiao, D. S. Wragg, P. S. Wheatley, I. L. Megson and R. E. Morris, *J. Am. Chem. Soc.*, 2008, **130**, 10440–10444.
38 Y. Liu, H. Kabbour, C. M. Brown, D. A. Neumann and C. C. Ahn, *Langmuir*, 2008, **24**, 4772–4777.
39 F. Bonino, S. Chavan, J. G. Vitillo, E. Groppo, G. Agostini, C. Lamberti, P. D. C. Dietzel, C. Prestipino and S. Bordiga, *Chem. Mater.*, 2008, **20**, 4957–4968.
40 J. G. Vitillo, L. Regli, S. Chavan, G. Ricchiardi, G. Spoto, P. D. C. Dietzel, S. Bordiga and A. Zecchina, *J. Am. Chem. Soc.*, 2008, **130**, 8386–8396.

41 S. Chavan, J. G. Vitillo, E. Groppo, F. Bonino, C. Lamberti, P. D. C. Dietzel and S. Bordiga, *J. Phys. Chem. C*, 2009, **113**, 3292–3299.
42 J. L. C. Rowsell and O. M. Yaghi, *J. Am. Chem. Soc.*, 2006, **128**, 1304–1315.
43 A. L. Spek, *J. Appl. Crystallogr.*, 2003, **36**, 7–13.
44 E. W. Lemmon, M. O. McLinden and D. G. Friend, Thermophysical Properties of Fluid Systems, in *NIST Chemistry WebBook, NIST Standard Reference Database Number 69*, ed. P. J. Linstrom and W. G. Mallard, National Institute of Standards and Technology, Gaithersburg MD, 20899.
45 S. R. Caskey, A. G. Wong-Foy and A. J. Matzger, *J. Am. Chem. Soc.*, 2008, **130**, 10870–10871.
46 K. S. Walton, A. R. Millward, D. Dubbeldam, H. Frost, J. J. Low, O. M. Yaghi and R. Q. Snurr, *J. Am. Chem. Soc.*, 2008, **130**, 406–407.
47 H. Wu, W. Zhou and T. Yildirim, *J. Am. Chem. Soc.*, 2009, **131**, 4995–5000.
48 W. Zhou, H. Wu, M. R. Hartman and T. Yildirim, *J. Phys. Chem. C*, 2007, **111**, 16131–16137.

This journal is © The Royal Society of Chemistry 2009